International Journal of Pharmaceutics 381 (2009) 40–48

Contents lists available at ScienceDirect

International Journal of Pharmaceutics

journal homepage: www.elsevier.com/locate/ijpharm

Self-assembled drug delivery systems. Part 4. *In vitro*/*in vivo* studies of the self-assemblies of cholesteryl-phosphonyl zidovudine

Yiguang Jin[a,b,*], Lei Xing[a,b], Ying Tian[a], Miao Li[a], Chunsheng Gao[c], Lina Du[a], Junxing Dong[a,**], Hongxuan Chen[b]

[a] *Department of Pharmaceutical Chemistry, Beijing Institute of Radiation Medicine, Beijing 100850, PR China*
[b] *Pharmaceutical College of Henan University, Kaifeng 475004, PR China*
[c] *Beijing Institute of Toxicology and Pharmacology, Beijing 100850, PR China*

ARTICLE INFO

Article history:
Received 11 May 2009
Received in revised form 8 July 2009
Accepted 22 July 2009
Available online 29 July 2009

Keywords:
Anti-HIV
Cholesterol
Phosphonate
Prodrugs
Self-assembly
Zidovudine

ABSTRACT

An amphiphilic prodrug of anti-HIV nucleoside analogue, cholesteryl-phosphonyl zidovudine (CPNZ) was synthesized. An aqueous suspension containing CPNZ self-assemblies was obtained through injecting the ethanol solution of CPNZ and cholesteryl succinyl poly(ethylene glycol) 1500 (20:1, mol/mol) into water under agitation. Hydrophobic interaction may be the driving force of molecular self-assembly. The self-assemblies were nanoscale with ~100 nm in size, and remained stable for a long time. Degradation of CPNZ self-assemblies was investigated in various environments including buffered solutions, plasma and rabbit tissue homogenates. CPNZ was degraded very slowly in neutral solutions but rapidly in various plasma with the half-lives ($t_{1/2}$) of less than 20 h. Tissue homogenates degraded CPNZ with varied rates depending on enzyme activity. CPNZ self-assemblies showed potent anti-HIV activity on MT4 cell model, the anti-HIV 50% effective concentration (EC_{50}) of which was 1 nM, only equal to 1/5 of AZT EC_{50}. CPNZ was rapidly eliminated from circulation and distributed into the mononuclear phagocyte system (MPS) including liver, spleen and lung after bolus intravenous administration of CPNZ self-assemblies followed slowly elimination. The possible products include AZT-5′-*H*-phosphonate, AZT and their derivatives. The MPS-targeted effect and high anti-HIV activity of CPNZ self-assemblies make them become a promising self-assembled drug delivery system (SADDS).

1. Introduction

Self-assembled drug delivery systems (SADDSs) have been explored in our lab since 2001, defined as self-assemblies of amphiphilic prodrugs, wherein three technologies, involving prodrug, molecular self-assembly, and nanotechnology are integrated (Jin et al., 2006). Compared with traditional drug carriers, SADDS can deliver themselves *in vivo* with the unique advantages of high drug loads, no drug leakage and controlled drug release at targets. However, some problems appeared in the previous researches. Although some of designed amphiphilic prodrugs occupy the self-assembling ability, their degradation is too slow to perform effective therapy (Jin et al., 2009). Therefore, when an amphiphilic prodrug is designed, it is necessary to simultaneously consider its self-assembling possibility in aqueous media, the stability of formed self-assemblies, and the degradation of prodrugs with the suitable rate at targets. However, it is very difficult to find an ideal prodrug.

We can now easily design and obtain the amphiphilic prodrugs to further form nanoscale self-assemblies to achieve tissue targeting. However, the controlling of degradation of prodrugs is difficult, mainly depending on molecular structures. The proper degradation of prodrugs should be modified based on the requirements of disease therapy. Generally, antiviral therapy requires rapid release of active drugs to reach the inhibitory concentration. There are many books and reviews to discuss metabolic hydrolysis and design of prodrugs (Testa and Mayer, 2003).

Antiviral nucleoside and nucleoside phosphonate drugs have played a significant role in improving the quality of life for many virally infected patients in recent years. Upon entering virally infected cells, these nucleosides and nucleoside phosphonates are phosphorylated to their active triphosphates or diphosphates, respectively, by nucleoside kinases. Therefore, the nucleoside phosphonate strategy is regarded as an effective approach to overcome viral resistance bypassing the first kinase. These phosphorylated species act as competitive inhibitors of reverse transcriptase and

* Corresponding author at: Department of Pharmaceutical Chemistry, Beijing Institute of Radiation Medicine, Beijing 100850, PR China. Tel.: +86 10 88215159; fax: +86 10 68214653.
** Corresponding author. Tel.: +86 10 66931314; fax: +86 10 68164257.
E-mail addresses: jin_yiguang@yahoo.com.cn (Y. Jin), dongjx@vip.sina.com (J. Dong).

0378-5173/$ – see front matter © 2009 Elsevier B.V. All rights reserved.
doi:10.1016/j.ijpharm.2009.07.024

as chain terminators, thus preventing viral replication. And these active polar-phosphate metabolites have prolonged intracellular half-lives (Hecker and Erion, 2008; Stella et al., 2007). It is noteworthy that two antiviral phosphonates are currently marketed, including adefovir dipivoxil for hepatitis B and tenofovir disoproxil for HIV. Furthermore, nucleoside phosphonates show higher polarity than nucleoside alone, which benefit to the design of amphiphilic prodrugs of SADDS.

Zidovudine (3′-azido-2′,3′-dideoxythymidine, AZT) is a potent inhibitor of HIV replication and the first clinically approved drug for AIDS. The major limitations of AZT chemotherapy are clinical toxicity that includes dose-related bone marrow suppression manifested as severe anaemia and leucopenia, hepatic abnormalities, myopathy, limited brain uptake, a short $t_{1/2}$ (~1 h) in plasma and the rapid development of drug resistance, resulting in administration of higher doses for maintaining therapeutic drug levels in plasma, thus further leading to bone marrow toxicity (Skoblov et al., 2004).

A series of AZT phosphonates were synthesized and anti-HIV activity was tested. They showed relatively high anti-HIV capability, and 2′,3′-dideoxy-3′-azidothymidine 5′-cyclohexylphosphite was the most active (Pokrovsky et al., 2001). 5′-(3′-Azido-3′-deoxythymidyl)hexanoyloxymethyl methylphosphonate was prepared as an anionic chemical delivery system for brain targeting. The phosphonate of AZT was hydrolyzed by esterases in the brain. The metabolic product, 5′-(3′-azido-3′-deoxythymidyl)methylphosphonate, could be locked in the brain due to anionic property (Somogyi et al., 1998).

Based on the above analysis, we designed and synthesized an amphiphilic *H*-phosphonate prodrug of AZT with the cholesteryl moiety as lipid tail to prepare SADDS. Self-assembly of the prodrug was explored and the formed self-assemblies were investigated on the *in vitro*/*in vivo* behaviors, involving characteristics, degradation, pharmacokinetics, tissue distribution, and anti-HIV activity.

2. Materials and methods

2.1. Materials

AZT was from Zhang Jiang Desano Science and Technology Co. Ltd., Shanghai, China. Organic solvents were of analytical grade. Other chemicals were of reagent grade. Distilled water was always used otherwise specially indicated. UV spectra, ^{1}H NMR (400 MHz) and ^{13}C NMR (100 MHz) spectra were recorded respectively on a Shimadzu UV-2501PC spectrophotometer, a JNM-ECA-400 NMR spectrometer, and ESI-MS were respectively recorded on a Thermo LCQ Advantage mass spectrometer.

MT4 cells and human immunodeficiency virus type-1 (HIV-1_{IIIB}) virus were from the Center of AIDS, Beijing Institute of Microbiology and Epidemiology. Plasma from BALB/c mice, Sprague–Dawley rats and albino rabbits was prepared in our lab. Plasma from beagle dogs and healthy human was donated by Prof. G. Dou of Beijing Institute of Transfusion Medicine.

Sprague–Dawley rats and albino rabbits from Laboratory Animal Center of Beijing Institute of Radiation Medicine (BIRM) were used. Principles in good laboratory animal care were followed and animal experimentation was in compliance with the Guidelines for the Care and Use of Laboratory Animals in BIRM. The rats and rabbits were sacrificed by euthanasia to remove tissues. The rat and rabbit tissue homogenates used in the experiments of chemical stability and tissue distribution were prepared in tissue/water (1:1, w/w).

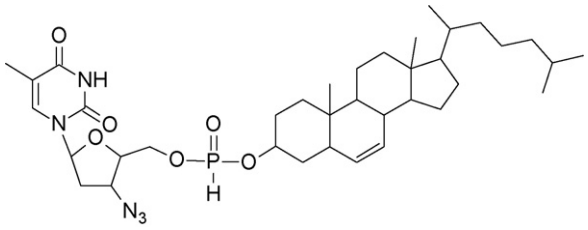

Fig. 1. Structure of cholesteryl-phosphonyl zidovudine (CPNZ).

2.2. Synthesis of cholesteryl-phosphonyl zidovudine

5′-Cholesteryl-phosphonyl zidovudine (CPNZ, AZT 5′-cholesteryl-*H*-phosphonate, $C_{37}H_{58}N_5O_6P$, Fig. 1) was synthesized according to the literature with a little change (Xiao et al., 2003). The brief procedure is described as follows. Cholesterol (5 mmol) was dissolved with anhydrous pyridine (10 ml). Diphenyl phosphonate (DPP, 5 mmol) was added and stirred for 26 h under room temperature in a sealed flask. The anhydrous pyridine solution of AZT (5 mmol in 10 ml) was dropped into the above reaction solution, and then stirred for an additional 12 h. Pyridine was removed by co-distillation with toluene under reduced pressure. After purification on a silica gel column (chloroform/ethanol, 50:1, v/v), CPNZ was obtained in high yield as white-like loose solid. TLC: cyclohexane/acetone, 1.1:0.9, v/v, R_f = 0.70; UV (EtOH): λ_{max} = 264.6 nm; δ_H (400 MHz, $CDCl_3$): 0.85 (6H, cholesteryl CH_3CHCH_3), 1.01–1.72 (32H, cholesteryl H), 1.95 (s, 3H, CH_3), 1.97 (1H, CH_2CHCH_2), 2.43–2.45 (m, 4H, 2′-CH), 4.30–4.38 (m, 4H, 5′-CH_2, 4′-CH, 3′-CH), 5.39 (1H, cholesteryl $CCHCH_2$), 6.22 (t, 1H, 1′-CH, $J_{1',2'}$ = 6.4 Hz), 7.38 (d, 1H, 6-CH), 7.27 (1H, PH), 9.13 (s, 1H, 3-CH); δ_C (100 MHz, $CDCl_3$): 18.62 (5-C-CH_3), 19.16–42.19 (22C, cholesteryl), 36.28 (2′-C), 49.80 ($CCHCH_2CH_2$), 59.93 ($CCHCHCH_3$), 59.98 (3′-C), 64.03 (5′-C), 77.86 ($OCHCH_2CH_2$), 82.09 (1′-C), 84.90 (4′-C), 111.56 (5-C), 123.68 (CH_2CCH), 135.26 (6-C), 138.53 (CH_2CCH), 150.29 (2-C), 163.78 (4-C); δ_P (160 MHz, $CDCl_3$): 7.23 (1P, J_{P-H} = 703 Hz); ESI-MS(+): 722.18 $(M+Na)^+$; ESI-MS(−): 698.21 $(M-H)^+$ (100), 699.28M^+ (44).

2.3. Preparation of self-assemblies in water

CPNZ is freely soluble in tetrahydrofuran (THF), like the other lipid derivatives of nucleoside antivirals (Jin et al., 2008). It is also freely soluble in ethanol with a high solubility of 100 mg/ml (143 mM), fit for the preparation of self-assemblies using the injection method. Cholesteryl succinyl poly(ethylene glycol) 1500 (CHS-PEG_{1500}, synthesized in our lab according to the literature (Yang et al., 2008)) was used as the unique additive. After exploring a variety of formulations and preparation processes, the optimal formulation and process for the ethanol injection method was found, described as follows. The ethanol solution containing CPNZ (5 mg/ml, 7.5 mM) with/without CHS-PEG_{1500} (0.72 mg/ml, 0.37 mM) was slowly injected into vortexed purified water by a microsyringe. The injecting process could be repeated for several times to get a homogeneous and slightly blue-scattering transparent suspension. After removing solvents and partial water by heat, a stable concentrated suspension of CPNZ self-assemblies was obtained with a high concentration up to more than 20 mg/ml CPNZ. The CHS-PEG_{1500}-containing suspension can be kept stable for more than one month at room temperature.

2.4. Characterization of self-assemblies

CPNZ self-assemblies were observed using a Philips CM120 80-kV transmission electron microscope (TEM). Five microliters of

CPNZ self-assemblies in suspensions were dropped onto carbon-coated copper nets and remained for one minute, and then mostly removed by filter paper from the edge of nets. A solution containing 2% sodium phosphotungstate (pH 6.5) was also dropped onto the above self-assemblies spread nets, and processed as the above. The resulted negative-stained samples were air-dried at room temperature, and moved to TEM for observation as soon as possible.

The dynamic lighting scattering method was used to measure the particle size and size distribution of self-assemblies on Zetasizer Nano ZS (Malvern, UK). The CPNZ self-assemblies-containing suspension was diluted with water until to about 0.1 mg/ml CPNZ, and then measured at 25 °C. The zeta potential of self-assemblies was also measured with the above instrument.

2.5. HPLC determination

HPLC experiments were performed on a Shimadzu 10Avp HPLC system (Japan), consisting of LC-10Avp pump, SPD-10Avp UV detector, SCL-10Avp controller, and Shimadzu CLASS-VP 6.12 chromatographic workstation software. The Diamonsil™ C18-ODS HPLC columns (5 μm, 250 mm × 4.6 mm) and the EasyGuard™ C18-ODS HPLC guard columns (5 μm, 8 mm × 4 mm) were purchased from Dikma Co., Ltd. (China). A manual injection valve and a 20-μl loop (7725i, Rheodyne, USA) were used. UV detector was fixed at 266 nm. The Heal Force® Super NW Water System (Shanghai Canrex Analytic Instrument Co. Ltd., China) was used to prepare purified water. When measuring the samples from biologics such as plasma, tissues, HPLC column temperature was kept at 30 °C with an AT-950 heater and cooler (Tianjin Automatic Science Instrument Co., Ltd.). CPNZ and its possible degradation product AZT were separately determined with the different mobile phases due to their significant polar differences. The mobile phases for CPNZ measurement was methanol/isopropanol/acetic acid (80/20/0.3, v/v/v) with the flow rate of 1.0 ml/min, and that for AZT measurement was methanol/water (35/65, v/v) at 0.8 ml/min. The retention times (t_R) of CPNZ and AZT were 8.7 min and 13.1 min, respectively.

2.6. Chemical stability of CPNZ

2.6.1. Stability in buffered solutions

Aliquots of 500 μl suspensions of CPNZ self-assemblies were diluted with 1.5 ml of various solutions at different pH values, including 0.1 and 0.01 M hydrochloride acid solutions (pH 1.0 and 2.0), 20 mM phosphate buffers (pH 5.0 and 7.4) and 20 mM Tris–HCl buffers (pH 9.0 and 12.0). The dilutions were incubated in a 37 °C bath. At predetermined time intervals, two replicates of 10 μl aliquots were removed, dissolved with 90 μl acetonitrile, mixed thoroughly, and separately assayed for CPNZ and AZT with HPLC.

2.6.2. Stability in plasma and tissue homogenates

Effects of animal and human plasma, and rabbit tissue homogenates on the chemical stability of CPNZ at 37 °C were also investigated with the similar procedures as above. CPNZ self-assemblies of 300 μl were mixed with 600 μl of plasma or tissue homogenates. At predetermined time intervals, two replicates of 10 μl aliquots were deproteinized with acetonitrile of 90 μl, followed by vortex for 5 min and centrifugation at 5000 × *g* for 10 min. The supernatants were separately determined for CPNZ and AZT with HPLC.

2.7. Anti-HIV effect on cell model

Anti-HIV effect of CPNZ self-assemblies was performed referred to our previous research (Jin et al., 2009). HIV-1_{IIIB} infected MT4 cells were used as model. CPNZ self-assemblies and AZT aqueous solutions were sterilized by film filtration with 0.22 μm filters. Drug samples were 10-fold diluted with the cultural media excluding serum. The concentration of CPNZ in cell cultures was from 10 μM to 0.1 nM, in six levels with a 10-fold decrease gradient and in triplicates every level. AZT aqueous solutions with the same concentration range and gradient as CPNZ were also investigated as control. After 72 h of incubation at 37 °C, the cytopathic effect (CPE) assay was performed with a light microscope and the 50% effective concentration (EC_{50}) was deduced.

2.8. Pharmacokinetics and tissue distribution in animals

Pharmacokinetics and tissue distribution of CPNZ were studied after bolus i.v. administration of CPNZ self-assemblies to rats and rabbits. The suspensions containing CPNZ self-assemblies of ~20 mg/ml were sterilized by 0.22 μm filters, and then injected into rats through tail vein or rabbits through ear vein. A dose of 40 mg/kg CPNZ was applied to rats, and 20 mg/kg to rabbits. About 0.3 ml of rat blood sample was collected from the opposite tail or ear veins of animals, and then put into heparinized centrifuge tubes at 1, 3, 5, 8, 10, 20, 30, 40, 50, 60, 90, 120, 240, 480, 960, 1440 min. Plasma was separated by centrifugation at 3000 rpm for 5 min, and then plasma of 50 μl was mixed with acetonitrile of 100 μl, followed by vortex, centrifuge at 5000 × *g* for 10 min and measurement by HPLC. In the tissue distribution experiments, rats were intravenously administered and sacrificed after 0.5, 2, 5, 10, 24 h, and the tissues were removed, weighted and disrupted to homogenates followed by the same procedure as plasma samples from the mixing process. Pharmacokinetics and tissue distribution of CPNZ in rabbits were also explored as above. Pharmacokinetic parameters are calculated with the 3p87 pharmacokinetic software supplied by Prof. H. Song of BIRM.

3. Results and discussion

3.1. Characteristics of CPNZ self-assemblies

CPNZ self-assemblies are nanoscale and spherical vesicles when CPNZ-alone is injected according to the TEM image (Fig. 2A). After doping CHS-PEG_{1500} in assemblies, the self-assemblies maintain vesicle morphology, although the size of vesicles increases from 83 nm of CPNZ-alone self-assemblies to 107 nm due to the longevity of PEG chains. Based on the TEM images (Fig. 2A and B), it is found that the vesicles are prone to aggregate, the basic reason of which is the relatively low negative surface charges with the zeta potential of −20.3 mV. It is well know that low surface charges, generally less than 30 mV of absolute value ($|\zeta|$) of zeta potential, could lead to particles unstable and then aggregate due to very high surface area if no other stabilizing mechanism is present (Heurtault et al., 2003; Wang et al., 2006).

Heating can lead to changes of self-assemblies. When the suspension of self-assemblies was concentrated by heat to remove water, aggregation of vesicles was improved. Single vesicle in the concentrated samples was bigger than that in the diluted suspensions, mainly resulting from fusion of aggregated vesicles (Fig. 2B and E). CPNZ-alone self-assembled vesicles are inclined to aggregate and fuse more seriously than the CPNZ/CHS-PEG_{1500} self-assembled vesicles upon heating. When heating at 100 °C was used to sterilize CPNZ-alone self-assemblies, all of vesicles disappeared and the replaced ones were unordered nanoparticles (Fig. 2C). However, most of vesicles were remained in CPNZ/CHS-PEG_{1500} assemblies (Fig. 2F). Therefore, it is demonstrated that CHS-PEG_{1500} can improve the physical stability of self-assemblies. The result is the same as stealth or sterically stabilized liposomes (Garbuzenko

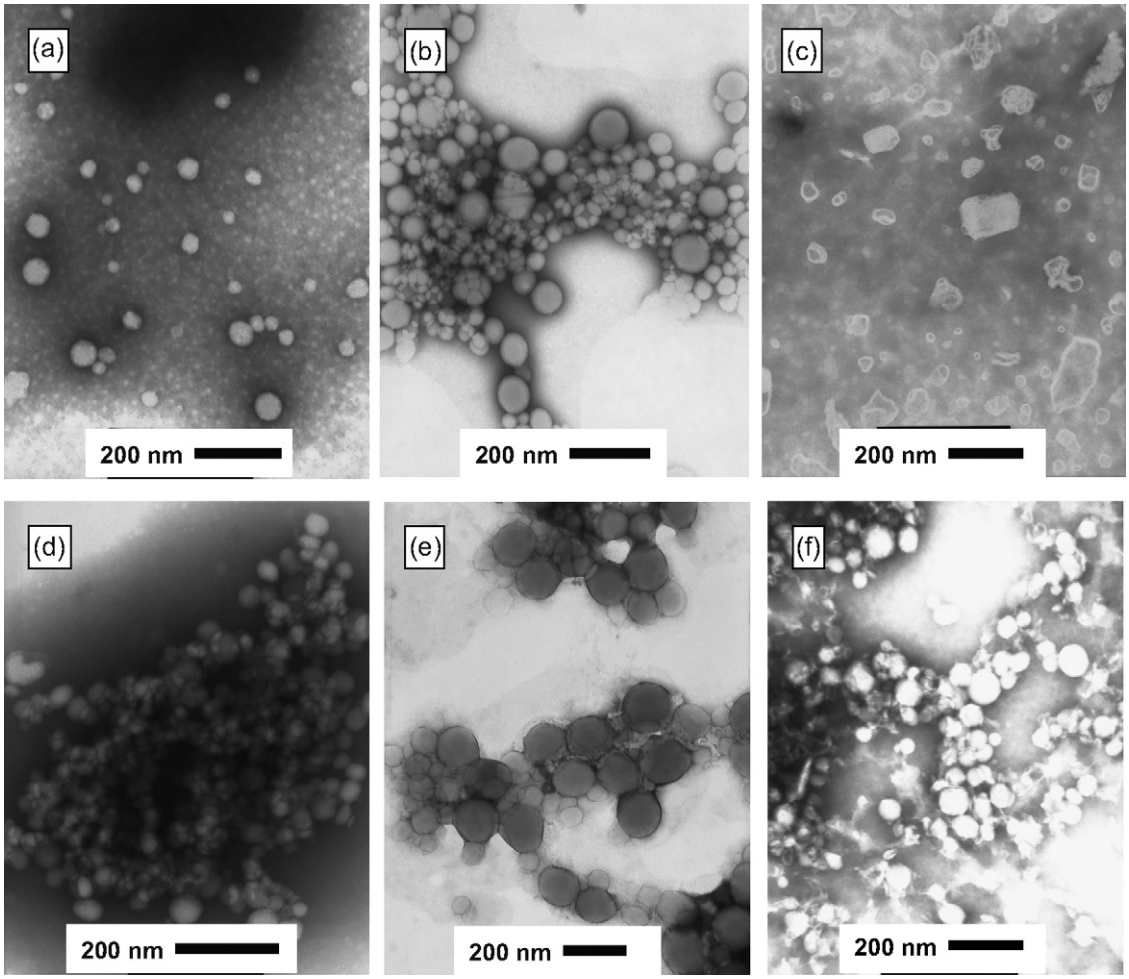

Fig. 2. TEM graphs of CPNZ self-assemblies. Graphs (A)–(C) represent the self-assemblies of CPNZ-alone, and graphs (D)–(F) represent the CPNZ/CHS-PEG_{1500} self-assemblies. The samples used in graphs (A) and (D) contained ~1.5 mg/ml CPNZ. The samples used in graphs (B) and (E) contained 10–20 mg/ml CPNZ after the concentrating process, and then they were heated at 100 °C for 30 min to obtain the samples used in graphs (C) and (F), respectively.

et al., 2005; Joannic et al., 1997; Sou et al., 2000). Long PEG chains coating on the surface of vesicles can protect particles from aggregating and fusing. This phenomenon is called steric stabilization. Based on the stability data, the mixture of CPNZ/CHS-PEG_{1500} (20:1, mol/mol) should be the optimal formulation to prepare CPNZ self-assemblies in the following research.

The driving force of CPNZ self-assembly is considered to be the hydrophobic interaction between the cholesteryl moieties of adjacent CPNZ molecules in the vesicle bilayers, the same as the other lipid derivatives of nucleoside antivirals in our previous research (Jin et al., 2008). There are two unique natures to lead to ethanol to be selected as solvents to dissolve CPNZ in the injection method. One is its high solubility for CPNZ. The other is the good water-miscible nature. High solubility of CPNZ in ethanol may result from hydrogen bonding between ethanol and the thymine and phosphonyl groups of CPNZ molecules, like other lipid nucleoside derivatives (Jin et al., 2008). When CPNZ molecules meet water upon injection, hydrophobic interaction between cholesteryl groups should immediately arise due to a lot of water surrounding them, and the primitive hydrogen bonds could be disrupted through water insertion and further replaced by the new hydrogen bonds between the polar heads of CPNZ and water molecules. The regulated amphiphilic prodrugs are inclined to self-assemble into bilayers in water with polar heads outside and lipid tails inside based on hydrophobic interaction, and then further bending of bilayers leads to formation of closed vesicles.

3.2. Degradation of CPNZ

3.2.1. Degradation in buffers and acid solutions

Appearance of the suspensions containing CNPZ self-assemblies did not show any change when they were mixed with the solutions at various pH values. However, degradation of the prodrug took place upon mixing, and the degradation rates were different depending on the pH values (Fig. 3). CPNZ rapidly degraded in the environments far away from neutral, i.e. pH 1.0 and 12.0, in this study. Dilution of the self-assemblies with the pH 12.0 buffered solution led to CPNZ degradation very fast (Fig. 3A), and the degradation product, AZT was also rapidly produced (Fig. 3B). Rapid degradation of the prodrug also happened in the pH 9.0 buffered solution though much slower than in pH 12.0. The other buffers led to weak degradation. Based on the pseudo-first degradation kinetics, the degradation $t_{1/2}$ of CPNZ are 11, 182, 315, 533, 52 and 6.7 h in pH 1.0, 2.0, 5.0, 7.4, 9.0 and 12.0, respectively. The neutral environment, i.e. pH 7.4, becomes the most stable condition. The relationship between pH values and degradation rate constants is showed in Fig. 4. Significantly, the prodrug can remain relatively stable in the neutral and weakly acidic environments. Therefore, the physical and chemical stability of CPNZ self-assemblies in aqueous suspensions can be guaranteed when preparing and storing them.

AZT-5′-*H*-phosphonate (phosphazid) might be one of hydrolysis products of CPNZ besides AZT. Phosphazid is also a prodrug

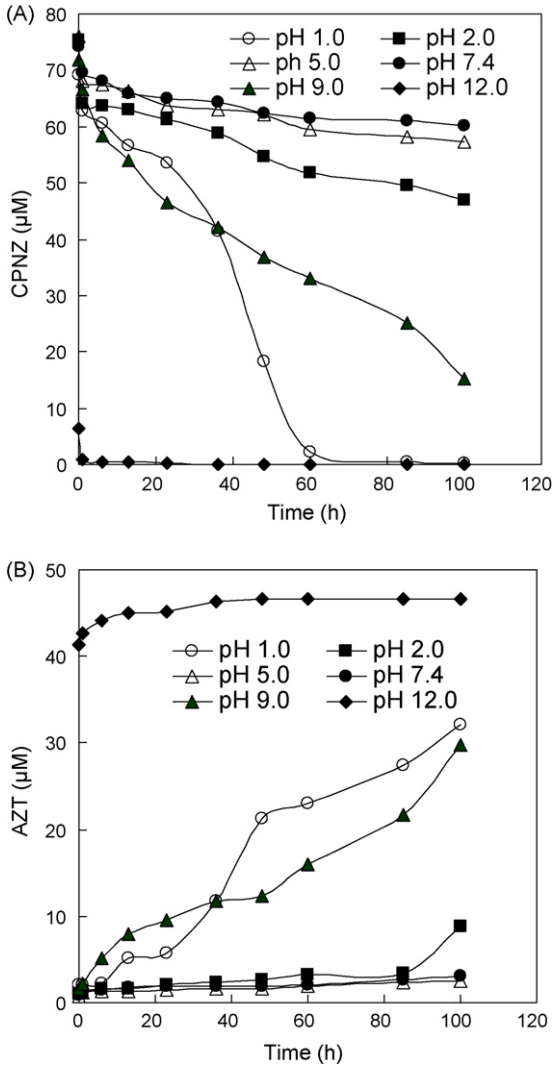

Fig. 3. Stability of CPNZ self-assemblies in a series of solutions with various pH values at 37 °C. Degradation of CPNZ was shown in diagram (A), and production of AZT was in diagram (B). The data are the mean of two replicated experiments.

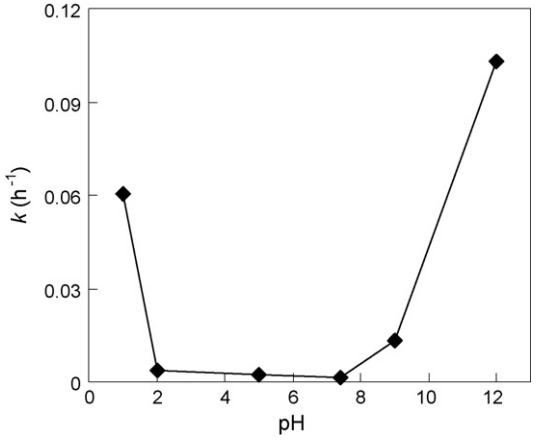

Fig. 4. The relationship between pH and degradation rate constants (k) of CPNZ in solutions.

of AZT, currently marketed in Russia in oral dosage form, under the brand name Nicavir. It has been the pre-clinical stage in the European Union and United States (Hoffmann and Mulcahy, 2007; Machado et al., 1999). In this study, it was found that the molar amount of produced AZT was less than that of disappeared CPNZ in buffered solutions. Therefore, phosphazid or phosphazid derivatives could be produced as the result of cleavage of the bond between cholesteryl and phosphonyl.

We also performed a control experiment by rapidly and directly mixing CPNZ solutions in dimethyl sulfoxide (DMSO) with the above buffered solutions. It was found that CPNZ in the DMSO/buffer suspensions was faster degraded than that in self-assemblies in the same pH solutions, and the $t_{1/2}$ of the former were 38 h in pH 9.0 and 4.2 h in pH 12.0. Because this simple mixing procedure was not controllable, most of CPNZ molecules should be in an unordered state not regulated bilayers like its self-assemblies. A great amount of sensitive phosphonyl ester bonds could be exposed to water so that degradation was speeded up. The result gives an evidence of the unique bilayer structure of CPNZ self-assemblies. The phosphonyl bonds hided in bilayers would be protected to a certain extent. In addition, the coating PEG chains could also hinder proton or hydroxyl ions closing (Taira et al., 2004). This phenomenon is also shown in our previous paper (Jin et al., 2006).

3.2.2. Degradation in plasma and tissue homogenates

The degradation of CPNZ in buffers, especially the neutral condition, is so slow that it is naturally worried whether the prodrug could be degraded *in vivo* to produce sufficient active forms. In our previous research, the hydrolysis of lipid carboxyl prodrugs was much faster in plasma and tissue homogenates than in buffers due to the presence of a great number of hydrolysis enzymes (Jin et al., 2006). However, it was also found that one amphiphilic prodrug, CSD, was very hard to be hydrolyzed even in plasma, resulting in no activity *in vitro* (Jin et al., 2009). Therefore, it is important to investigate the degradation of CPNZ in biological environments.

CPNZ was rapidly degraded and AZT was also greatly produced in plasma from various resources, involving mouse, rats, human, rabbit and dog (Fig. 5), the $t_{1/2}$ of which were 3.4, 3.7, 4.2, 4.5 and 6.3 h in the above turn, much faster than that in neutral buffered solutions (e.g., pH 7.4). Degradation of CPNZ and production of AZT in rabbit tissue homogenates was also rapid (Fig. 6), the $t_{1/2}$ of which were 33, 1.2, 2.1, 10, 10, 4.7 and 3.2 h, respectively, in the homogenates from heart, liver, spleen, lung, kidney, brain and testis. Rapid degradation of CPNZ in plasma and tissue homogenates is tightly relevant to the presence of a great amount of hydrolysis enzymes, and it is well known that enzymatic hydrolysis is generally much faster than chemical hydrolysis.

Many types of hydrolysis enzymes might be responsible for the degradation of CPNZ, involving phosphodiesterase, alkaline phosphatase and carboxylesterase (Fux et al., 2008; Kelly et al., 1975; Somogyi et al., 2004). In addition, there was an enzyme capable to specially hydrolyze phosphonates, considered as a phosphonate esterase (Han et al., 1992). Therefore, it is not difficult to understand the rapid degradation of CPNZ in plasma and tissue homogenates. In the above described case, the very slow degradation of CSD in human plasma was shown with the $t_{1/2}$ of 990 h, the essential reason of which was confirmed to be the hard hydrolyzed cholesteryl-acyl bond (Jin et al., 2009). The relatively rapid degradation of CPNZ highly related to its unique molecular structure, demonstrates that the design of prodrug is close to a success though the *in vitro*/*in vivo* studies should be further performed. Based on the data of degradation (Fig. 5), the plasma of rats and rabbits had the similar degradation capability as human plasma so that rats and rabbits were selected as model animals in the following *in vivo* investigation.

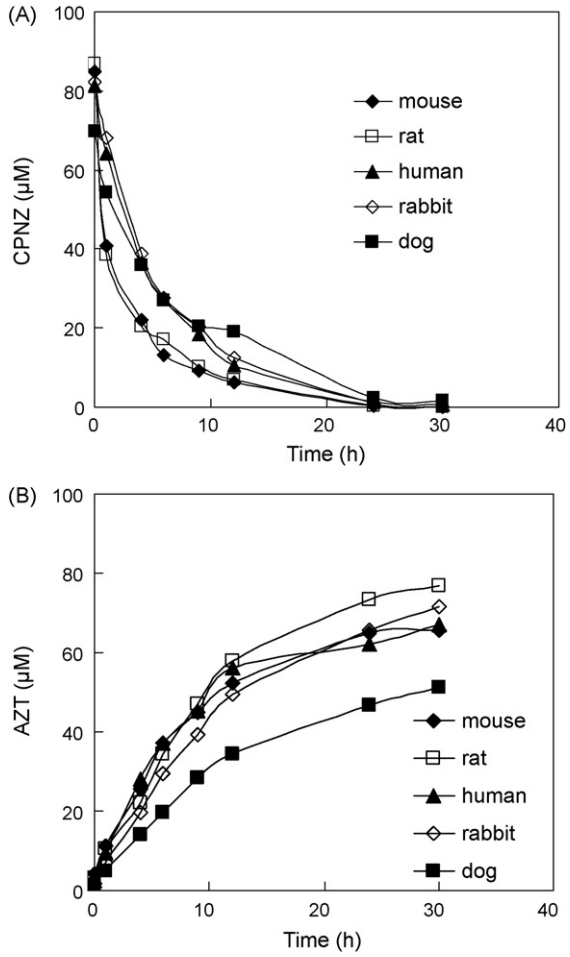

Fig. 5. Stability of CPNZ self-assemblies in plasma at 37 °C. Degradation of CPNZ was shown in diagram (A), and production of AZT was in diagram (B). The data are the mean of two replicated experiments.

Interestingly, CPNZ has significant different degradation profiles in plasma compared with tissue homogenates. The molar amount of produced AZT is nearly equal to that of disappeared CPNZ in various plasmas (Fig. 5). However, there are marked differences between the molar amount of disappeared CPNZ and that of produced AZT in rabbit tissue homogenates. Furthermore, the differences depend on the types of tissues. In the homogenates from heart, kidney, brain and testis, the molar amount of disappeared CPNZ is about 2- or 3-folds of produced AZT. However, in liver, spleen and lung that are the main organs of the mononuclear phagocyte system (MPS), the fold values can be up to 4–7. In fact, cholesteryl ester hydrolase present in macrophages could degrade CPNZ to cholesterol and AZT-5′-*H*-phosphonate (von Eckardstein, 1996; Zhao et al., 2008, 2007). Therefore, more complicated metabolism of CPNZ could happen in macrophages than other cells and plasma. The difference of enzymes in various rabbit tissue homogenates should lead to the different metabolism of CPNZ. The production of AZT-5′-*H*-phosphonate and its derivatives would benefit to antiviral therapy based on the above description. In addition, AZT may be transformed to other metabolites. Besides the phosphorylation of AZT through thymidine kinase and other kinases, leading to production of monophosphate, diphosphate and triphosphate, AZT glucuronide and 3′-amino-3′-deoxythymidine (AMT) are also produced by glucuronyl transferase and CYP450/P450-reductase, respectively (Veal and Back, 1995).

3.3. In vitro antiviral activity of CPNZ self-assemblies

The anti-HIV EC_{50} of CPNZ self-assemblies on MT4 cell model is 1 nM in this study, which is only 1/5 of the EC_{50} (5 nM) of AZT in the control experiment. Therefore, it could be concluded that CPNZ is a potent anti-HIV agent. The reason for the high activity could involve many aspects. First, the freely dispersing and nanoscale CPNZ self-assemblies have a lot of chances to contact the surface of cells. Second, CNPZ molecules in endosomes or lysosomes easily escape through biomembranes due to the high lipophilicity of prodrugs. Third, CPNZ could be degraded to AZT-5′-*H*-phosphonate and AZT in cellular plasma, and then perform sufficient anti-HIV action. This exciting result provides a promising perspective of anti-HIV therapy *in vivo*.

The nucleoside phosphonates strategy is regarded as an effective prodrug bypassing the first kinase as described in Section 1. One of possible metabolites of CPNZ, AZT-5′-*H*-phosphonate (phosphazid) probably plays an important role in anti-HIV treatment. In a report about the *in vitro* anti-HIV-1 experiment of phosphazid, the EC_{50} of phosphazid was 36 nM though the value was 2 nM for AZT (Machado et al., 1999). Another report showed that the EC_{50} of phosphazid was 130 nM though 14 nM for AZT (Pokrovsky et al., 2001). The authors found that alkyl

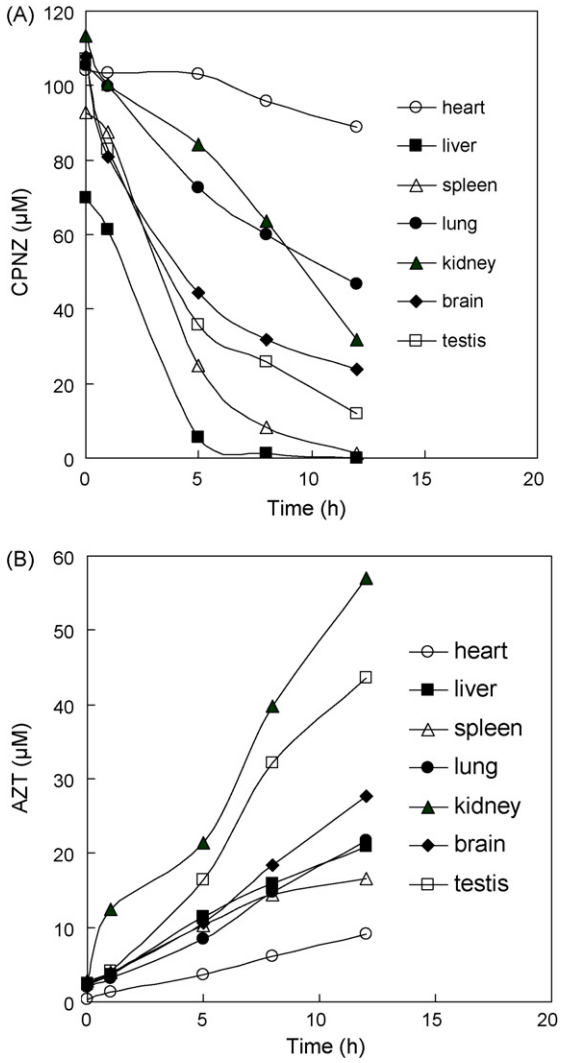

Fig. 6. Stability of CPNZ self-assemblies in rabbit tissue homogenates at 37 °C. Degradation of CPNZ was shown in diagram (A), and production of AZT was in diagram (B). The data are the mean of two replicated experiments.

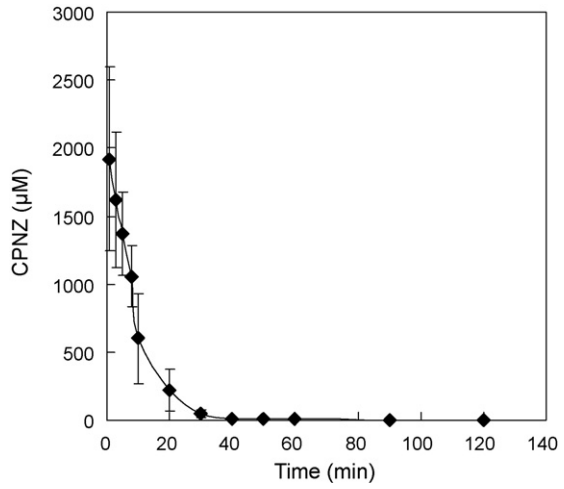

Fig. 7. The time profile of CPNZ concentration in plasma after bolus i.v. administration of CPNZ self-assemblies to rats ($n = 5$).

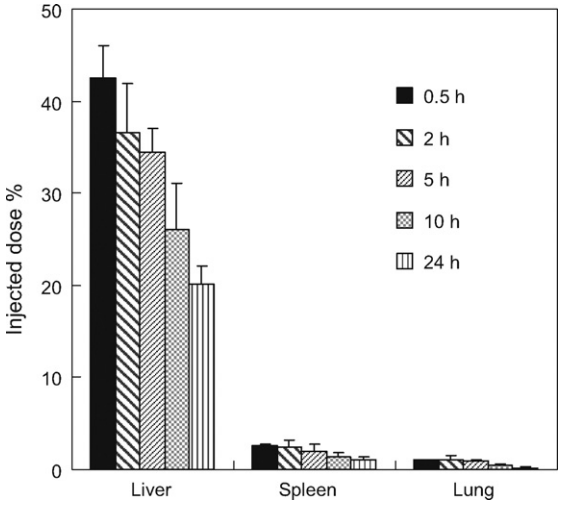

Fig. 9. The tissue distribution of CPNZ after bolus i.v. administration of CPNZ self-assemblies to rats ($n = 3$).

derivatives of AZT-5′-*H*-phosphonate showed a markedly different antiviral activity. The EC_{50} of them were 13, 110, 24.9 and 2.4 nM for isopropyl, adamantyl, isopentyl and cyclohexyl derivatives, respectively, wherein the cyclohexyl derivative, i.e. 2′,3′-dideoxy-3′-azidothymidine-5′-cyclohexylphosphite, had the highest anti-HIV activity. Significantly, lipophilicity increased the antiviral activity of derivatives of AZT-5′-*H*-phosphonate except for the adamantyl derivative due to its large steric space. These lipophilic derivatives could penetrate cell membranes more easily than the high polar phosphazid, resulting in a high concentration in the cell to perform good antiviral action. Unlike the above lipophilic AZT phosphates, CPNZ self-assemblies own both high dispersing and lipophilic natures, rationally leading to higher activity than lipophilic AZT derivatives alone.

3.4. Pharmacokinetics and tissue distribution of CPNZ self-assemblies

Rapid elimination of CPNZ from circulation happened after bolus i.v. administration of the self-assemblies to rats and rabbits (Figs. 7 and 8), in agreement with the pharmacokinetics of other colloidal systems due to immune response (Torchilin, 2006). Other SADDS previously prepared by us also show the similar pharmacokinetic behavior (Jin et al., 2009, 2006). Based on the pharmacokinetic profile in rats (Fig. 7), the 0–8 min range is considered as the distribution phase with the $t_{1/2\alpha}$ of 4.2 min. In the profile in rabbits (Fig. 8), the $t_{1/2\alpha}$ of the 0–10 min distribution phase is 4.4 min. The values are a little longer than the distribution $t_{1/2\alpha}$ (1.5 min) of another SADDS (SGSA self-assembled nanoparticles) in rabbits (Jin et al., 2006). This little long circulating effect should result from the CHS-PEG_{1500} coating though the assertion of pegylated lipids is not sure. Pegylated lipids can also increase the circulating time of liposomes or nanoparticles although the effect is influenced by many factors (Awasthi et al., 2003; Moghimi et al., 2001; Moghimi and Szebeni, 2003). One SADDS, CSD self-assembled nanoparticulates coated by poloxamers also show a long circulating effect (Jin et al., 2009). Only a little AZT was found in the blood of rats and rabbits within 0.5 h of administration because of the rapid distribution of prodrugs into the MPS (see the following text), and the short elimination of AZT from circulation.

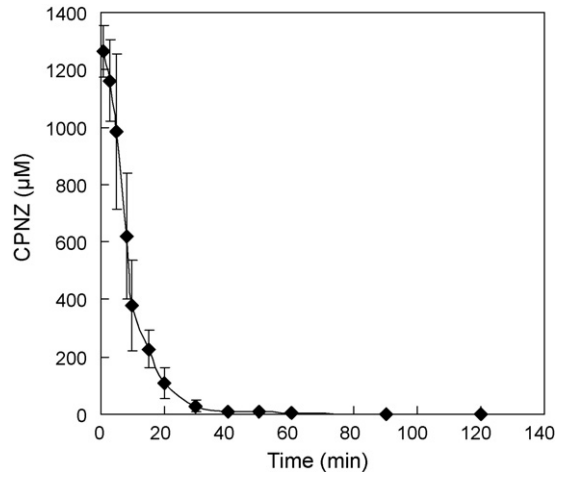

Fig. 8. The time profile of CPNZ concentration in rabbit plasma after bolus i.v. administration of CPNZ self-assemblies to rabbits ($n = 5$).

The *in vivo* fate of CPNZ self-assemblies was further explored through measuring drug distribution in tissues including liver, spleen, lung, heart, kidney, brain, and testis of rats and rabbits. The MPS including liver, spleen and lung are still the main distribution tissues of CPNZ in rats and rabbits, in agreement with the site-specific distribution behavior of other colloidal systems (Ishida et al., 2002; Moghimi et al., 2001). The concentration of CPNZ in rat liver reached a high level of 207 μg/g at 0.5 h after administration, while 197 μg/g in spleen and 37 μg/g in kidney. Only a little CPNZ was detected in rat kidney, about 2.48 μg/g, and less CPNZ was found in brain and testis. No CPNZ was detected in rat heart. When rabbits were as model, CPNZ concentrations in liver, spleen, lung, kidney and testis were 160, 270, 33, 2.8 and 1.2 μg/g at 0.5 h after administration. Only a very little CPNZ was detected in rabbit brain, and no CPNZ in heart.

Rat liver was the main accumulating site of CPNZ, and the amount of prodrugs in liver was very high, equal to 43% of the total administered dose at 0.5 h (Fig. 9). The value was 51% in rabbit liver (Fig. 10). The prodrug was slowly eliminated from the targeted rat tissues, and the elimination $t_{1/2}$ were 25, 16 and 8 h in liver, spleen and lung, respectively, based on the pseudo-first order kinetics. In the case of rabbits, the elimination $t_{1/2}$ were 22, 11, 7.5 h in liver, spleen and lung, respectively. Furthermore, only a little AZT, about 1 μg/g or more, was detected within 48 h of administration in the main targeted tissues of rats and rabbits.

Compared with the degradation of CPNZ in tissue homogenates, the $t_{1/2}$ of CPNZ in the targeted organs are much longer than those

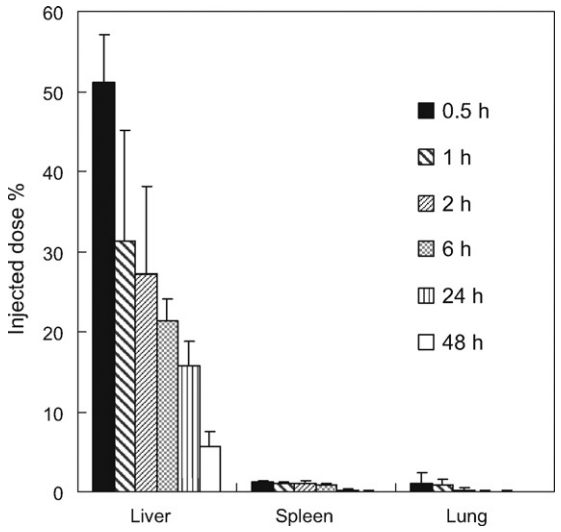

Fig. 10. The tissue distribution of CPNZ after bolus i.v. administration of CPNZ self-assemblies to rabbits ($n = 3$).

in the corresponding homogenates except for lung. The elimination $t_{1/2}$ in the rabbit liver is almost equal to 20-folds of the degradation $t_{1/2}$ in the rabbit liver homogenate, and about 5-folds in the case of spleen. The unique interpretation of the differences could be the marked difference in amount and types of enzymes released in homogenates and existed in the targeted cellular organelle (e.g., phagosomes). Generally, the *in vivo* environment should be more complicated than *in vitro*. Other reports also show that there is a difference of enzyme activity between *in vitro* and *in vivo* (Sintov et al., 2002; Tobin et al., 2006). Even in various organelles of macrophages, the amount and activity of hydrolases are also different (Claus et al., 1998). Maybe more enzymes responsible for the degradation of CPNZ were released from other cellular organelles than phagosomes when homogenizing tissues with water.

In addition to the $CD4^+$ T lymphocytes, cells of the MPS also play a decisive role as a reservoir for HIV. Because of the important role of cells of the monocyte/macrophage lineage in the pathogenesis of HIV, fully effective anti-HIV therapy must reach in addition to other target cells (Aquaro et al., 2002; Bender et al., 1996). Many anti-HIV agents-loaded nanocarriers were prepared for targeting of the MPS, such as liposomes (Duzgunes et al., 1999; Gagne et al., 2002; Pretzer et al., 1997), polymer nanoparticles (Bender et al., 1996), lipid nanoparticles (Dou et al., 2007), PEG-coating nanocarriers (Wan et al., 2007), mannosylated gelatin nanoparticles (Jain et al., 2008), dendrimer (Dutta et al., 2007). All nucleoside analogues inhibitors of HIV-reverse transcriptase have the potent efficacy in macrophages. Nevertheless, the limited penetration of some of them, coupled with the scarce phosphorylation ability of macrophages, suggests that nucleoside analogues carrying preformed phosphate or phosphonate groups may have a potential role against HIV replication in macrophages. This hypothesis is supported by the great anti-HIV activity of tenofovir and other acyclic nucleoside phosphonates in macrophages that may provide a rationale for the remarkable efficacy of tenofovir in HIV-infected patients (Aquaro et al., 2002).

In this study, CPNZ self-assemblies have been demonstrated to be a potent anti-HIV agent *in vitro*, and mainly distribute into the MPS *in vivo*. Therefore, CPNZ self-assemblies as one SADDS would possibly become a promising macrophage-targeted anti-HIV nanomedicine.

4. Conclusions

A promising SADDS was prepared in this study. An amphiphilic prodrug of anti-HIV nucleoside analogue zidovudine, CPNZ, has the self-assembling capability, forms the stable and nanoscale CPNZ self-assemblies in water with the relatively fast degradation in biological environments, and shows the high anti-HIV activity and the targeting of the MPS followed by degradation at the targeted organs. Referred to the standards of successful SADDS (Jin et al., 2009), CPNZ self-assemblies may be regarded as an approximately successful SADDS. In the future research, the anti-HIV efficiency of CPNZ self-assemblies will be detected on animal models.

Acknowledgements

This work was supported by the National Natural Science Foundation of China (No. 30672542) and The National Key Technologies R&D Program for New Drugs (No. 2009ZX09301-002). We acknowledge Prof. Jingyun Li and Ms. Siyang Liu for the help of the *in vitro* anti-HIV experiment. We thank Helen Qing Zhang for the help of English writing.

References

Aquaro, S., Calió, R., Balzarini, J., Bellocchi, M.C., Garaci, E., Perno, C.F., 2002. Macrophages and HIV infection: therapeutical approaches toward this strategic virus reservoir. Antiviral Res. 55, 209–225.

Awasthi, V.D., Garcia, D., Goins, B.A., Phillips, W.T., 2003. Circulation and biodistribution profiles of long-circulating PEG-liposomes of various sizes in rabbits. Int. J. Pharm. 253, 121–132.

Bender, A.R., Briesen, H.V., Kreuter, J., Duncan, I.B., Rubsamen-Waigmann, H., 1996. Efficiency of nanoparticles as a carrier system for antiviral agents in human immunodeficiency virus-infected human monocytes/macrophages in vitro. Antimicrob. Agents Chemother. 40, 1467–1471.

Claus, V., Jahraus, A., Tjelle, T., Berg, T., Kirschke, H., Faulstich, H., Griffiths, G., 1998. Lysosomal enzyme trafficking between phagosomes, endosomes, and lysosomes in J774 macrophages. Enrichment of cathepsin H in early endosomes. J. Biol. Chem. 273, 9842–9851.

Dou, H., Morehead, J., Destache, C.J., Kingsley, J.D., Shlyakhtenko, L., Zhou, Y., Chaubal, M., Werling, J., Kipp, J., Rabinow, B.E., Gendelman, H.E., 2007. Laboratory investigations for the morphologic, pharmacokinetic, and anti-retroviral properties of indinavir nanoparticles in human monocyte-derived macrophages. Virology 358, 148–158.

Dutta, T., Agashe, H.B., Garg, M., Balasubramanium, P., Kabra, M., Jain, N.K., 2007. Poly(propyleneimine) dendrimer based nanocontainers for targeting of efavirenz to human monocytes/macrophages in vitro. J. Drug Targeting 15, 89–98.

Duzgunes, N., Pretzer, E., Simoes, S., Slepushkin, V., Konopka, K., Flasher, D., De Lima, M.C.P., 1999. Liposome-mediated delivery of antiviral agents to human immunodeficiency virus-infected cells. Mol. Membr. Biol. 16, 111–118.

Fux, C.A., Rauch, A., Simcock, M., Bucher, H.C., Hirschel, B., Opravil, M., Vernazza, P., Cavassini, M., Bernasconi, E., Elzi, L., Furrer, H., 2008. Tenofovir use is associated with an increase in serum alkaline phosphatase in the Swiss HIV Cohort Study. Antivir. Ther. 13, 1077–1082.

Gagne, J.-F., Desormeaux, A., Perron, S., Tremblay, M.J., Bergeron, M.G., 2002. Targeted delivery of indinavir to HIV-1 primary reservoirs with immunoliposomes. Biochim. Biophys. Acta 1558, 198–210.

Garbuzenko, O., Barenholz, Y., Priev, A., 2005. Effect of grafted PEG on liposome size and on compressibility and packing of lipid bilayer. Chem. Phys. Lipids 135, 117–129.

Han, G.-Y., Fan, X.-H., Jin, X.-B., Wang, D.-P., 1992. Specific detection and properties of enzyme hydrolyzing phosphonate ester in serum. Clin. Chem. 38, 377–380.

Hecker, S.J., Erion, M.D., 2008. Prodrugs of phosphates and phosphonates. J. Med. Chem. 51, 2328–2345.

Heurtault, B., Saulnier, P., Pech, B., Proust, J.-E., Benoit, J.-P., 2003. Physico-chemical stability of colloidal lipid particles. Biomaterials 24, 4283–4300.

Hoffmann, C., Mulcahy, F., 2007. ART 2007/2008: the horizon and beyond. In: Hoffmann, C., Rockstroh, J.K., Kamps, B.S. (Eds.), HIV Medicine 2007. Flying Publisher, Paris, pp. 127–159.

Ishida, T., Harashima, H., Kiwada, H., 2002. Liposome clearance. Biosci. Rep. 22, 197–224.

Jain, S.K., Gupta, Y., Jain, A., Saxena, A.R., Khare, P., Jain, A., 2008. Mannosylated gelatin nanoparticles bearing an anti-HIV drug didanosine for site-specific delivery. Nanomed. Nanotech. Biol. Med. 4, 41–48.

Jin, Y., Ai, P., Xin, R., Tian, Y., Dong, J., Chen, D., Wang, W., 2009. Self-assembled drug delivery systems. Part 3. In vitro/in vivo studies of the self-assembled nanoparticulates of cholesteryl acyl didanosine. Int. J. Pharm. 368, 207–214.

Jin, Y., Tong, L., Ai, P., Li, M., Hou, X., 2006. Self-assembled drug delivery systems. 1. Properties and in vitro/in vivo behavior of acyclovir self-assembled nanoparticles (SAN). Int. J. Pharm. 309, 199–207.

Jin, Y., Xin, R., Ai, P., Chen, D., 2008. Self-assembled drug delivery systems. 2. Cholesteryl derivatives of antiviral nucleoside analogues: synthesis, properties and the vesicle formation. Int. J. Pharm. 350, 330–337.

Joannic, R., Auvray, L., Lasic, D.D., 1997. Monodisperse vesicles stabilized by grafted polymers. Phys. Rev. Lett. 78, 3402–3405.

Kelly, S.J., Dardinger, D.E., Butler, L.G., 1975. Hydrolysis of phosphonate esters catalyzed by 5′-nucleotide phosphodiesterase. Biochemistry 14, 4983–4988.

Machado, J., Salomon, H., Oliveira, M., Tsoukas, C., Krayevsky, A.A., Wainberg, M.A., 1999. Antiviral activity and resistance profile of phosphazid—a novel prodrug of AZT. Nucleosides Nucleotides Nucleic Acids 18, 901–906.

Moghimi, S.M., Hunter, A.C., Murray, J.C., 2001. Long-circulating and target-specific nanoparticles: theory to practice. Pharmacol. Rev. 53, 283–318.

Moghimi, S.M., Szebeni, J., 2003. Stealth liposomes and long circulating nanoparticles: critical issues in pharmacokinetics, opsonization and protein-binding properties. Prog. Lipid Res. 42, 463–478.

Pokrovsky, A.G., Pronayeva, T.R., Fedyuk, N.V., Shirokova, E.A., Khandazhinskaya, A.L., Tarusova, N.B., Karpenko, I.L., Krayevsky, A.A., 2001. Anti-HIV activity of novel phosphonate derivatives of AZT, d4T, and ddA. Nucleosides Nucleotides Nucleic Acids 20, 767–769.

Pretzer, E., Flasher, D., Duzgunes, N., 1997. Inhibition of human immunodeficiency virus type-1 replication in macrophages and H9 cells by free or liposome-encapsulated L-689,502, an inhibitor of the viral protease. Antiviral Res. 34, 1–15.

Sintov, A.C., Behar-Canetti, C., Friedman, Y., Tamarkin, D., 2002. Percutaneous penetration and skin metabolism of ethylsalicylate-containing agent. TU-2100: in-vitro and in-vivo evaluation in guinea pigs. J. Control. Release 79, 113–122.

Skoblov, Y., Karpenko, I., Shirokova, E., Popov, K., Andronova, V., Galegov, G., Kukhanova, M., 2004. Intracellular metabolism and pharmacokinetics of 5′-hydrogenphosphonate of 3′-azido-2′,3′-dideoxythymidine, a prodrug of 3′-azido-2′,3′-dideoxythymidine. Antiviral Res. 63, 107–113.

Somogyi, G., Buchwald, P., Bodor, N., 2004. Metabolic properties of phosphonate esters. Pharmazie 59, 378–381.

Somogyi, G., Buchwald, P., Nomi, D., Prokai, L., Bodor, N., 1998. Targeted drug delivery to the brain via phosphonate derivatives. II. Anionic chemical delivery system for zidovudine (AZT). Int. J. Pharm. 166, 27–35.

Sou, K., Endo, T., Takeoka, S., Tsuchida, E., 2000. Poly(ethylene glycol)-modification of the phospholipid vesicles by using the spontaneous incorporation of poly(ethylene glycol)-lipid into the vesicles. Bioconjugate Chem. 11, 372–379.

Stella, V.J., Borchardt, R.T., Hageman, M.J., Oliyai, R., Maag, H., Tilley, J.W., 2007. Prodrugs: Challenges and Rewards. Springer, Dordrecht.

Taira, M.C., Chiaramoni, N.S., Pecuch, K.M., Alonso-Romanowski, S., 2004. Stability of liposomal formulations in physiological conditions for oral drug delivery. Drug Deliv. 11, 123–128.

Testa, B., Mayer, J.M., 2003. Hydrolysis in Drug and Prodrug Metabolism: Chemistry, Biochemistry, and Enzymology. Verlag Helvetica Chimica Acta, Zürich, Switzerland.

Tobin, P., Clarke, S., Seale, J.P., Lee, S., Solomon, M., Aulds, S., Crawford, M., Gallagher, J., Eyers, T., Rivory, L., 2006. The in vitro metabolism of irinotecan (CPT-11) by carboxylesterase and beta-glucuronidase in human colorectal tumours. Br. J. Clin. Pharmacol. 62, 122–129.

Torchilin, V.P., 2006. Nanoparticulates as Drug Carriers. Imperial College Press, London.

Veal, G.J., Back, D.J., 1995. Metabolism of zidovudine. Gen. Pharmac. 26, 1469–1475.

von Eckardstein, A., 1996. Cholesterol efflux from macrophages and other cells. Curr. Opin. Lipidol. 7, 308–319.

Wan, L., Pooyan, S., Hu, P., Leibowitz, M.J., Stein, S., Sinko, P.J., 2007. Peritoneal macrophage uptake, pharmacokinetics and biodistribution of macrophage-targeted PEG-fMLF (N-formyl-methionyl-leucyl-phenylalanine) nanocarriers for improving HIV drug delivery. Pharm. Res. 24, 2110–2119.

Wang, L., Wang, K., Santra, S., Zhao, X., Hilliard, L.R., Smith, J.E., Wu, Y., Tan, W., 2006. Watching silica nanoparticles glow in the biological world. Anal. Chem. 78, 646–654.

Xiao, Q., Ju, Y., Yang, X., Zhao, Y.-F., 2003. Electrospray ionization mass spectrometry of AZT H-phosphonates conjugated with steroids. Rapid Commun. Mass Spectrom. 17, 1405–1410.

Yang, D.-b., Zhu, J.-b., Huang, Z.-j., Ren, H.-x., Zheng, Z.-j., 2008. Synthesis and application of poly(ethylene glycol)-cholesterol (Chol-PEG^m) conjugates in physicochemical characterization of nonionic surfactant vesicles. Colloids Surf. B: Biointerf. 63, 192–199.

Zhao, B., Song, J., Ghosh, S., 2008. Hepatic overexpression of cholesteryl ester hydrolase enhances cholesterol elimination and in vivo reverse cholesterol transport. J. Lipid Res. 49, 2212–2217.

Zhao, B., Song, J., St Clair, R.W., Ghosh, S., 2007. Stable overexpression of human macrophage cholesteryl ester hydrolase results in enhanced free cholesterol efflux from human THP1 macrophages. Am. J. Physiol. Cell Physiol. 292, C405–C412.